Thin Solid Films 556 (2014) 211–215

Contents lists available at ScienceDirect

Thin Solid Films

journal homepage: www.elsevier.com/locate/tsf

Synthesis of a cuprite thin film by oxidation of a Cu metal precursor utilizing ultrasonically generated water vapor

Myo Than Htay *, Masahiko Okamura, Ryo Yoshizawa, Yoshio Hashimoto, Kentaro Ito

Department of Electrical and Electronic Engineering, Faculty of Engineering, Shinshu University, 4-17-1 Wakasato, Nagano 380-8553, Japan

ARTICLE INFO

Article history:
Received 25 April 2013
Received in revised form 27 January 2014
Accepted 29 January 2014
Available online 6 February 2014

Keywords:
B1. Cu_2O
B1. Cuprous oxide
B1. Cuprite
A3. Ultrasonic spray pyrolysis
A3. Water decomposition
A3. Oxidation

ABSTRACT

A Cu_2O thin film of cuprite crystal structure was fabricated via a decomposition reaction of water vapor generated by ultrasonic vibration. The thin film, which was grown on a soda-lime glass substrate at 530 °C, exhibited a prominent (111) preferred orientation with an optical bandgap of about 2.1 eV and resistivity of 2.81×10^4 Ω cm. Generation of H_2 gas during the reaction process contributed to suppressing the growth of impurity tenorite phase. In a conventional process of thermal oxidation, the formation of the cuprite phase was always accompanied by that of the tenorite phase due to an excess oxygen exposure near the surface of the films.

1. Introduction

A cuprous oxide, Cu_2O, is an abundant and nontoxic p-type semiconductor with a direct bandgap of E = 2.172 eV at 0 K [1,2]. Due to its characteristic properties, it is known as a promising material for applications to the hetero-junction devices such as diodes, photovoltaic cells, etc. [3–9]. A pure cuprite phase of Cu_2O was synthesized mainly by means of thermal oxidation at a temperature higher than 1000 °C [10–15]. This is because a monoclinic tenorite phase of cupric oxide, CuO, that has quite a different material property is usually mixed in the cuprite phase of Cu_2O when prepared at oxidation temperatures lower than 1000 °C under atmospheric oxygen pressure [15–17]. Owing to this issue, the application of Cu_2O was limited to the devices in which the use of high temperature fabrication process could be allowed. In order to overcome this, it is necessary to develop a low temperature synthesizing process so that the choice of counter material and the substrate for fabrication of the hetero-junction device will become more flexible. To date, various fabrication techniques to obtain a single phase cuprous oxide at low temperatures such as sputtering, pulsed laser deposition, etc. were reported [18–23]. However, achieving a reproducible pure cuprite phase of Cu_2O was still a challenge. Here, in this paper, we report a technique to prepare a pure cuprite phase of Cu_2O thin film on a soda-lime glass substrate at temperatures lower than 600 °C. In this technique, thin films with the pure cuprite phase were achieved in a reproducible manner just by controlling the decomposing temperature of ultrasonically generated water vapor.

2. Experimental details

A thin film of Cu precursor was deposited on a soda-lime glass (SLG) substrate by vacuum evaporation of Cu metal (99.999% purity). Deionized water was used as an oxidation agent and its vapor was generated by the ultrasonic vibration of 2.4 MHz. The generated vapor was transported to a heated precursor located in a reaction chamber by means of N_2 carrier gas. The flow rate of water vapor was adjusted at 1 L/min. The oxidation of Cu or the decomposing reaction of water vapor was carried out in our original ultrasonic spray pyrolysis system. In this system, an infrared-gold-image furnace (ULVAC, E-25) was used, where the samples to be oxidized were placed inside a graphite susceptor for heating. The structural detail of the system was described in our previous report [24]. Before and after oxidation processes, a pre-evacuation and post-evacuation of the reaction chamber were carried out in order to purge unintended oxygen contamination of the ambient during the heating and cooling periods. An X-ray diffractometry (XRD, Rigaku, RINT-2200 V/PCSV, Cu $K\alpha$ ray; $\lambda = 1.5418$ Å with a Bragg–Brentano $\theta - 2\theta$ geometry at 40 kV, 30 mA) was used for identification of the crystalline properties of the films. For evaluating the surface morphology of the films, a field emission scanning electron microscope (FE-SEM, Hitachi, S-4100) was used. A four-probe method (Kyowa Riken, K89PS, Pt coated tungsten carbide probes with 1 mm gap) was applied for measuring the resistivity of the samples in rectangular shape of 15×10 mm^2 in size. A heat-probe method was used to determine the conductivity type of the films. A spectrophotometer (Shimadzu UV-3100) was used to measure the transmittance and the optical bandgap of the films. An X-ray photoelectron spectroscope (XPS, Surface Science Instruments, S-probe 7339, Al $K\alpha$ 1486.6 eV source

* Corresponding author. Tel.: +81 26 269 5241; fax: +81 26 269 5220.
E-mail address: myoth@shinshu-u.ac.jp (Myo Than Htay).

0040-6090/$ – see front matter
http://dx.doi.org/10.1016/j.tsf.2014.01.077

with a hemispherical energy analyzer) was used to evaluate the composition and depth profiling of the samples. During the depth profiling measurements, sputtering of the samples was carried out by an Ar^+ ion sputter gun (Leybold–Heraeus 867–918) operated at the beam energy of 2 keV and beam current of 8 μA. Calibration of the binding energy scale was performed by referencing the values of Au $4f_{7/2}$ and Cu $2p_{3/2}$ spectra measured under the same condition. The Raman spectra were collected on a laser Raman spectrometer (RENISHAW, inVia Reflex 785S, an excitation source of λ = 532 nm, 450 mW, and a 1800 line mm^{-1} grating).

3. Results and discussion

The XRD patterns of samples oxidized by water vapor at various temperatures are shown in Fig. 1(a) to (e). The decomposition reaction of water was carried out for 30 min to obtain each oxidized film. It was found that the intensity of an XRD reflection peak due to the (111) crystal plane of cuprite Cu_2O becomes stronger as the reaction temperature is elevated from 450 to 530 °C. On the contrary the intensity of a (111) reflection peak due to cubic copper is decreased as the oxidation of the copper precursor layer proceeds and vanished completely at 530 °C. The results indicate that the rate of oxidation was much faster at the reaction temperature of 530 °C than that of 450 °C. At 530 °C, only diffraction peaks due to the cuprite phase of Cu_2O thin film but no peaks belong to the cubic copper of precursor and tenorite phase of CuO were obtained as shown in Fig. 1(c). The film exhibited a strong diffraction peak due to the (111) plane of the cuprite phase. The diffraction peak due to the (200) plane of the cuprite phase is also observed in a moderate intensity. This suggested that the Cu metal precursor was completely oxidized to form a pure cuprite film, which was strongly oriented with the (111) plane parallel to the substrate. In the samples prepared at higher temperatures such as 550 °C and 580°, the intensity of the (111) peak due to the Cu_2O phase appeared weaker than that of 530 °C, while the peak of (111) plane of Cu metal precursor was still remained and its intensity was stronger at higher reaction temperatures above 530 °C. From these results, it may be considered that the higher the temperature was, the slower the oxidation rate. The reason for the slow oxidation rate could be related to the existence of reduction reaction of Cu_2O phase into the Cu metal under the ambient containing activated hydrogen generated from decomposed water vapor at higher temperatures. In Fig. 2, the XRD patterns of the samples prepared at 530 °C for various reaction periods are shown. The formation of Cu_2O phase was confirmed in all the samples. A pure cuprite phase was achieved in the samples prepared at the reaction period of 30 and

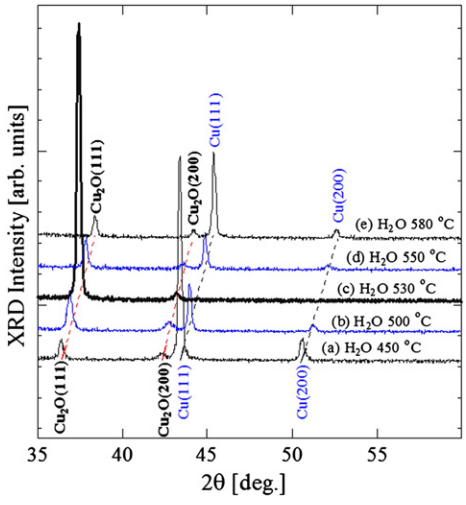

Fig. 1. The XRD patterns of the samples prepared at (a) 450 °C, (b) 500 °C, (c) 530 °C, (d) 550 °C, and (e) 580 °C by water vapor.

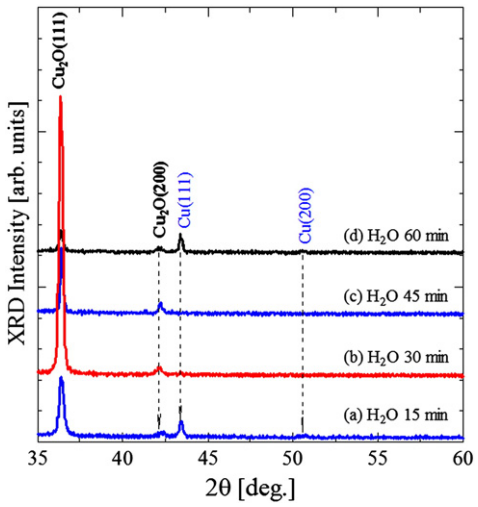

Fig. 2. The XRD patterns of the samples prepared at 530 °C for various reaction periods of (a) 15 min, (b) 30 min, (c) 45 min, and (d) 60 min by water vapor.

45 min as shown in Fig. 2(b) and (c). The crystalline quality was better for the sample with shorter reaction period of 30 min. In the sample oxidized for 15 min, peaks due to the Cu metal of the precursor were still remained as shown in Fig. 2(a), implying that the reaction period was not enough. In the case of the sample prepared at the longest reaction period of 60 min, the diffraction peak due to the (111) plane of Cu metal was detected again in addition to that of the Cu_2O phase. This result suggested that the complete oxidation of a Cu metal precursor to form a pure Cu_2O film is observed between 30 and 45 min of reaction, and beyond that period the reduction of the Cu_2O phase back into the Cu metal has taken place. This reduction phenomenon was similar to the cases prepared at 550 °C and higher as discussed above. The formation of the tenorite phase of CuO was not observed under any preparation conditions pertaining to this technique. This is an astonishing result, since an excess amount of oxygen was supplied from water vapor and the process in this experiment was operated under the condition that might favor the formation of the CuO phase rather than the Cu_2O if one takes into account the pressure vs temperature phase stability diagram of Cu–Cu_2O–CuO system reported in the literatures [8,11,14,15,17].

The surface morphology and the cross-sectional images of the sample prepared at 530 °C for 30 min are shown in Fig. 3(a) and (b). It was found that the crystal grains in the form of an equilateral triangular pyramid with a flat top were arranged in various orientations over the whole surface of the continuous Cu_2O thin film. From this structural appearance, it is reasonable to assume that each pyramidal structure corresponds to a single crystal grain of the cubic crystal of cuprite phase. The dimensions of these single crystal grains were varied between 300 and 1000 nm. It was observed that most of the pyramidal grains are oriented with the (111) crystallographic planes of the equilateral triangle shape parallel to the surface of the film. The geometry of the equilateral triangular planes perpendicular to the [111] axis of the cubic cuprite lattice is depicted in Fig. 3(c). This microscopic observation was in good agreement with the result of XRD pattern of Fig. 1(c): the strong (111) peak is due to reflection from the (111) faces of the equilateral triangular shape of the Cu_2O phase as shown in Fig. 3(c). The lattice constants of the cubic crystal evaluated from the XRD data of this sample are estimated as $a = b = c = 4.27$ Å, in good agreement with previous data [2]. The thickness of the Cu_2O film obtained after the oxidation process was about 400 nm which is nearly two times as thick as that of the Cu precursor. The film showed a p-type conductivity with resistivity of $2.81 \times 10^4 \Omega$ cm, which is in the same order to the reported value for pure Cu_2O phase [25]. Its optical bandgap was estimated to be about 2.1 eV by the $(\alpha h\nu)^2 vs\ h\nu$ plot as shown in

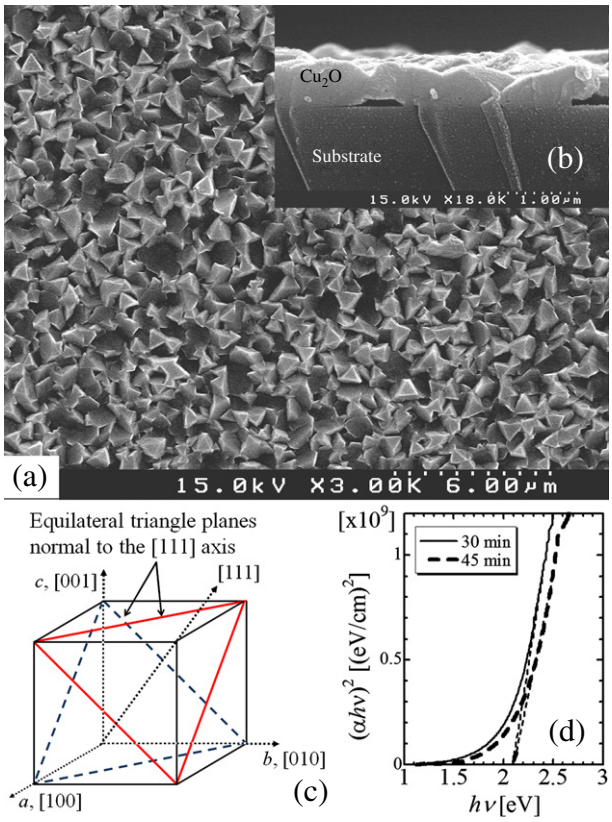

Fig. 3. (a) SEM image of the surface morphology of the cuprite thin film prepared at 530 °C for 30 min by ultrasonically generated water vapor, (b) the corresponding cross-sectional image of (a), (c) a unit lattice of the cubic crystal showing the geometry of the equilateral triangle planes perpendicular to the [111] axis of cuprite crystal phase, and (d) estimation of the optical bandgap of the samples prepared at 530 °C for 30 min and 45 min.

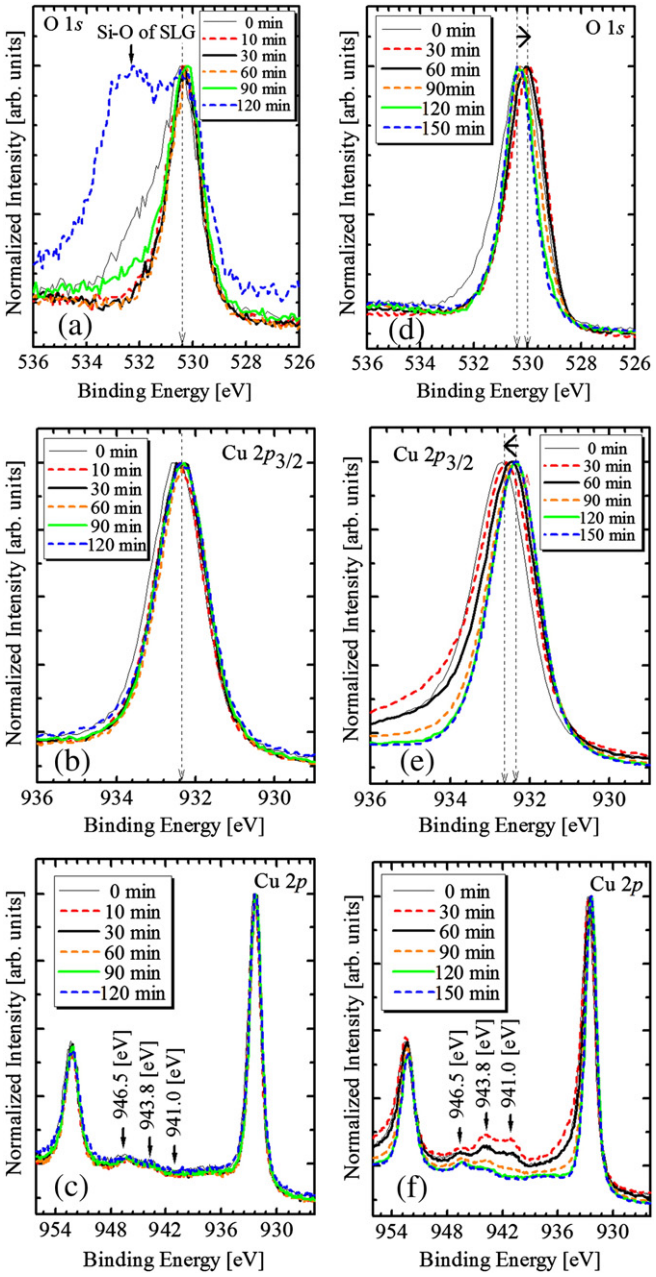

Fig. 4. XPS spectra of (a) O 1*s*, (b) Cu $2p_{3/2}$, (c) Cu 2*p* measured from the sample which has pure cuprite phase (left column), and the right column shows the XPS spectra of (d) O 1*s*, (e) Cu $2p_{3/2}$, (f) Cu 2*p* detected from the sample which has both cuprite and tenorite phases. All the spectra are normalized to the corresponding peak height.

Fig. 3(d). It was revealed by XPS analysis that the film had almost the same stoichiometric composition as the Cu_2O phase, i.e., Cu = 66.5 at.% and O = 33.5 at.%. The detail structure of O 1*s* and Cu 2*p* spectra are shown in Fig. 4(a) to (c). It was clarified that the composition of the sample was homogenous throughout the entire depth of the film. We have confirmed that the sample consists of a pure cuprite phase because there is neither chemical shift nor structural difference of the O 1*s* peak at 530.4 eV and the Cu $2p_{3/2}$ peak at 932.4 eV due to the impurity phases such as CuO and $Cu(OH)_2$ in the whole film [2,26]. A broad shoulder around 532.4 eV of the O 1*s* spectrum, which could be assigned as the Si – O bond of the SLG substrate, was observed at the back side of the film. The unusual spectrum shape detected at the surface (sputtering time: 0 min) of the film was due to the surface contamination. In Fig. 5(a), a Raman spectrum of the sample, which exhibited only the Cu_2O phase by the XRD and XPS analysis, is shown. It is clear that the Raman shifts appear around 110, 148, 218, 416, and 634 cm^{-1} are due to the Cu_2O phase alone [27,28]. This result also gives a strong evident of the formation of a pure Cu_2O phase.

$$2Cu(s) + H_2O(vapor) \rightleftharpoons Cu_2O(s) + H_2(g) \quad (1)$$

$$4Cu(s) + O_2(g) \rightarrow 2Cu_2O(s) \quad (2)$$

$$2Cu_2O(s) + O_2(g) \leftrightarrows 4CuO(s) \quad (3)$$

To clarify the growth phenomenon observed in this experiment, the fundamental reactions responsible for this process are suggested in Eqs. (1) to (3). The main reaction may include equilibrium between oxidation of the Cu metal by H_2O and reduction of the Cu_2O by H_2 decomposed from the vapor as shown in Eq. (1). In this equilibrium, temperature is a major factor to determine which reaction is more favorable. Normally, when heated water vapor and Cu metal encounter at relatively low temperatures, a chemical reaction from the left to the right hand side of Eq. (1) could be prominent at the surface of precursor to form a Cu_2O film. In this reaction, the oxygen decomposed from water will be consumed, while the remaining hydrogen gas will be released as a byproduct. The oxidation reaction of Cu with O_2, which results in the formation of the Cu_2O phase, may be simply expressed by Eq. (2). If there were excess oxygen gas, further reaction of Cu_2O phase with O_2 as described in Eq. (3) proceeding from the left to the right hand side might have continued so that the formation of a CuO phase takes place at its surface. After the reaction that generates H_2 gas, a well-known strong reduction agent, the reduction reaction as

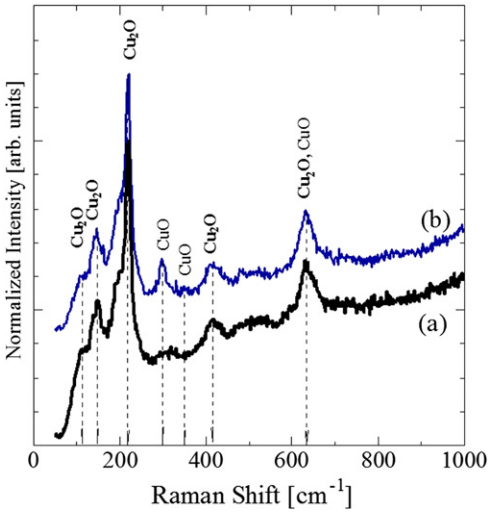

Fig. 5. Raman spectra of (a) the sample which has a pure cuprite phase and (b) the sample which has both the cuprite and tenorite phases measured at room temperature. All the spectra are normalized to the corresponding peak height.

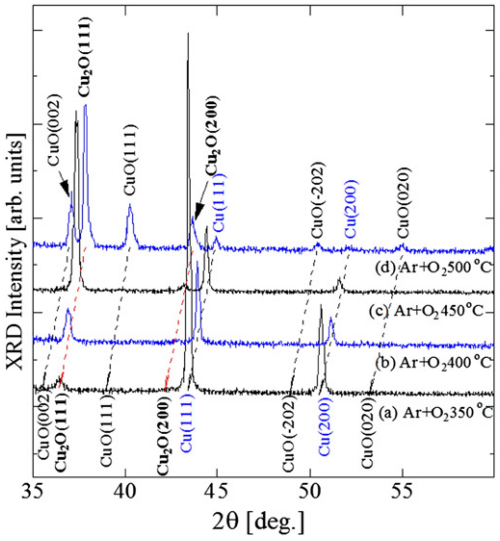

Fig. 6. The XRD patterns of the samples prepared at (a) 350 °C, (b) 400 °C, (c) 450 °C, and (d) 500 °C by a gas mixture of Ar + O_2.

shown in Eq. (1) proceeding from the right to the left hand side might also take place in addition to the oxidation reaction until equilibrium is established at the corresponding temperature. In the experimental results discussed above, the high yield of the Cu_2O phase at 530 °C can be best explained by the forward reaction of Eq. (1). The reaction path expressed in Eq. (3) is considered ineffective because the formation of the CuO phase was not observed under any conditions. The growth of the CuO phase is possibly suppressed by the presence of the hydrogen gas. The experimental finding that there is indeed a reduction reaction between Cu_2O and H_2 was reported in the reference [29]. In addition to the reduction reaction, the dissociation of CuO phase as shown in the Eq. (3) proceeding from the right to the left hand side might also be prominent at temperatures higher than 530 °C so that the oxidation rate was relatively slow [16,30]. As a consequence, further oxidation of cuprous oxide could be prevented by the presence of a reducing agent in the ambient, resulting in the growth of pure cuprite thin films. If the temperature of oxidation of the Cu or the decomposition of the water vapor is carefully adjusted in order to achieve a high yield in the generation of H_2 gas, this fabrication method could also be applied for extracting a valuable H_2 gas as a byproduct at relatively low temperature.

For comparison, the conventional thermal oxidation of a Cu precursor was carried out by using a gas mixture of 98% Ar and 2% O_2. The O_2 partial pressure of the ambient was maintained at 16 Pa and the reaction period was set to 60 min in this experiment. This condition was considered to be in a pressure range where the formation of the CuO phase is prevalent [8,11,14,15,17]. The XRD patterns of samples prepared at the temperatures between 350 and 500 °C are shown in Fig. 6(a) to (d). It is evident from the result that the (111) peak of Cu_2O phase was increased but that of the Cu precursor was reduced when the reaction temperature was raised from 350 to 450 °C. No CuO phase was detected but the Cu metal was still remained in these samples. This tendency was similar to the case of oxidation process using water vapor at the same 450 °C discussed above, although the oxidation rate was relatively slower. However, for the sample prepared at 500 °C, a CuO phase was detected in addition to the Cu_2O phase as shown in Fig. 6(d). Both (111) peaks of Cu and Cu_2O in the sample shown in Fig. 6(d) were still remained but weaker in intensity compared to that of the sample shown in Fig. 6(c). Therefore, it is considered that further oxidation of the Cu_2O phase into the CuO phase as shown in Eq. (3) proceeding from the left to the right hand side was now more favorable than the oxidation of Cu shown in Eq. (2). In other words, the formation of CuO phase is predominant to the formation of Cu_2O phase during the later period of reaction in this conventional thermal oxidation process. In a clear contrast to the case where water vapor was used at 500 °C, the conventional thermal oxidation at the same temperature resulted in the formation of both CuO and Cu_2O phases [see Figs. 1(b) and 6(d)]. Because there was no reduction agent such as H_2 in the conventional thermal oxidation, further oxidation of Cu_2O phase into CuO phase could exist near the surface and the formation of the CuO phase was unavoidable even if there was an excess Cu metal that remained underneath.

Another experiment of thermal oxidation of Cu precursors (200 nm in thickness) was carried out at 450 °C under O_2 partial pressure of 2.66 Pa for various reaction periods to investigate the formation timing of CuO phase during the oxidation reaction. The XRD intensities of the (111) peaks of Cu, Cu_2O, and CuO are shown in Fig. 7 as a function of reaction period. It was observed that when the reaction period increased, the intensity of (111) peak of Cu was decreased and finally diminished at the reaction period of 67 min. The intensity of (111) peak of Cu_2O phase was increased initially and then was decreased after 65 min accompanied by the formation of CuO phase. The diffraction peak of CuO kept increasing even beyond the period when the Cu metal precursor was completely oxidized and the peak of the Cu_2O phase was decreasing. These results suggested that the formation of the Cu_2O phase is a predominant reaction over that of the CuO formation during the initial period, and then after 65 min of the reaction

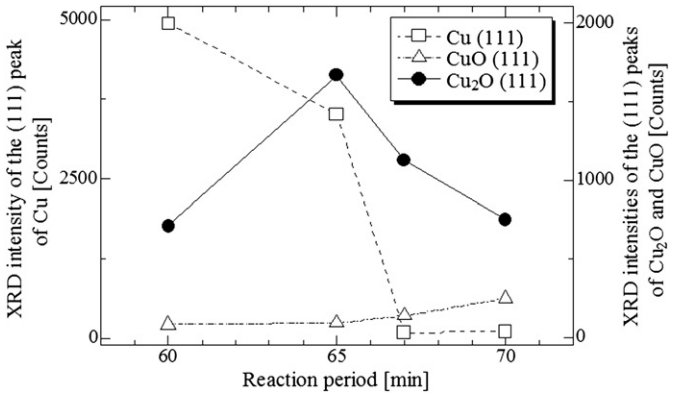

Fig. 7. The transformation of XRD intensities of the (111) peaks of Cu, Cu_2O, and CuO phases versus the reaction periods of the samples prepared by thermal oxidation at 450 °C under O_2 partial pressure of 2.66 Pa.

period, the CuO formation process over taken that of the Cu_2O phase formation, although Cu metal was still remained underneath. In other words, transformation of the Cu_2O phase into the CuO phase becomes a major reaction after the growth of a moderate thickness of Cu_2O phase near the surface. When the thermal oxidation for various reaction periods was carried out at the temperatures lower than 450 °C, similar tendency for the formation of CuO phase at the late reaction period was also observed but the growth rate was much slower. The XPS depth profile of the sample, which has both the Cu_2O and CuO phases, is shown in Fig. 4(d) to (f). The O 1*s* spectrum obtained near the surface exhibited the chemical shift toward low binding energy side in reference to the inner region of the film. In contrast, the Cu $2p_{3/2}$ spectrum showed an opposite shift and the peak width was relatively broad. The changes in the structure of the multiple satellite peaks located between the Cu $2p_{1/2}$ (952.2 eV) and Cu $2p_{3/2}$ (932.4 eV) peaks were also obvious. It was reported that these multiple satellite peaks of the cuprite phase exhibit a different structure from those of the tenorite phase [2]. The peaks at 946.5 eV and 943.8 eV are usually detected in the cuprite phase and the peaks at 943.8 eV and 941.0 eV are attributed to the tenorite phase. In Fig. 4(f), the peaks at 943.8 eV and 941.0 eV were strong near the surface and were weak at the bottom side. These results indicate that the tenorite crystal phase, which is transformed from the cuprite phase by the forward reaction as shown in Eq. (3), is localized near the surface of the film but the intact cuprite phase remains underneath the film. The existence of CuO phase was also confirmed by the Raman spectrum as shown in Fig. 5(b). The Raman shifts around 297, 345, and 629 cm^{-1} due to the CuO phase, which is not detected in the samples prepared by utilizing water vapor, are clearly observed along with the peaks due to the Cu_2O phase as shown in Fig. 5(a) [31]. This is also consistent with the results of XRD and XPS analysis discussed above.

4. Conclusions

A thin film consisting of pure cuprite phase of Cu_2O was fabricated on a soda-lime glass substrate at relatively low temperature of 530 °C by the reaction of a copper metal precursor with water vapor produced via ultrasonic vibration. The thin film showed p-type conduction with an optical bandgap of about 2.1 eV and resistivity of $2.81 \times 10^4\ \Omega$ cm. By using water vapor as an oxidation agent, the generation of H_2 gas during the oxidation reaction could contribute to suppressing the formation of the impurity tenorite phase of CuO so that a pure cuprite thin film of Cu_2O was grown at the temperatures lower than 600 °C. The effect of reduction reaction was obvious at the high reaction temperatures as well as at a later stage of film growth. In the case of conventional thermal oxidation, the formation of the impurity tenorite phase near the surface of the film was unavoidable under the excess oxygen ambient.

Acknowledgments

Part of this work was supported by a Grant-in-Aid for Young Scientists (B) of Grant number (23710088) from the Japan Society for the Promotion of Science. Special thanks are due to Mr. Isamu Minemura for his help in this study.

References

[1] C. Kittel, Introduction to Solid State Physics, seventh ed. Wiley, New York, 1996. 201.
[2] J. Ghijsen, L.H. Tjeng, J. van Elp, H. Eskes, J. Westerink, G.A. Sawatzky, M.T. Czyzyk, Phys. Rev. B 38 (1988) 11322.
[3] B. Kramm, A. Laufer, D. Reppin, A. Kronenberger, P. Hering, A. Polity, B.K. Meyer, Appl. Phys. Lett. 100 (2012) 094102.
[4] D. Kim, H.S. Shin, J.Y. Song, Appl. Phys. Express 5 (2012) 085001.
[5] T. Minami, Y. Nishi, T. Miyata, J. Nomoto, Appl. Phys. Express 4 (2011) 062301.
[6] F.Y. Hsu, S.J. Liu, Y.I. Lu, L.Y. Chen, H.W. Fang, Jpn. J. Appl. Phys. 48 (2009) 035501.
[7] G.K. Paul, Y. Nawa, H. Sato, T. Sakurai, K. Akimoto, Appl. Phys. Lett. 88 (2006) 141901.
[8] A.E. Rakhshani, Solid State Electron. 29 (1986) 7.
[9] J. Mizuguchi, Jpn. J. Appl. Phys. 15 (1976) 907.
[10] N.N. Greenwood, J.S. Anderson, Nature 164 (1949) 346.
[11] T. Ito, H. Yamaguchi, K. Okabe, T. Masumi, J. Mater. Sci. 33 (1998) 3555.
[12] A. Kinoshita, T. Nakano, Jpn. J. Appl. Phys. 5 (1966) 1121.
[13] T. Nakano, K. Ohtani, A. Kinoshita, T. Okuda, Jpn. J. Appl. Phys. 3 (1964) 124.
[14] W.S. Brower Jr., H.S. Parker, J. Cryst. Growth 8 (1971) 227.
[15] R.D. Schmidt-Whitley, M. Martinez-Clemente, A. Revcolevschi, J. Cryst. Growth 23 (1974) 113.
[16] F.H. Smyth, H.S. Roberts, J. Am. Chem. Soc. 42 (1920) 2582.
[17] H.S. Roberts, F.H. Smyth, J. Am. Chem. Soc. 43 (1921) 1061.
[18] A. Chen, H. Long, X. Li, Y. Li, G. Yang, P. Lu, Vacuum 83 (2009) 927.
[19] S. Ishizuka, T. Maruyama, K. Akimoto, Jpn. J. Appl. Phys. 39 (2000) L786.
[20] T. Kosugi, S. Kaneko, J. Am. Ceram. Soc. 81 (1998) 3117.
[21] T. Maruyama, Sol. Energy Mater. Sol. Cells 56 (1998) 85.
[22] H. Matsumura, A. Fujii, T. Kitatani, Jpn. J. Appl. Phys. 35 (1996) 5631.
[23] Z. Blank, W. Brenner, Nature 222 (1969) 79.
[24] M.T. Htay, Y. Hashimoto, K. Ito, Jpn. J. Appl. Phys. 46 (2007) 440.
[25] L.D.L.S. Valladares, D.H. Salinas, A.B. Dominguez, D.A. Najarro, S.I. Khondaker, T. Mitrelias, C.H.W. Barnes, J.A. Aguiar, Y. Majima, Thin Solid Films 520 (2012) 6368.
[26] M.C. Biesinger, L.W.M. Lau, A.R. Gerson, R. St. C. Smart, Appl. Surf. Sci. 257 (2010) 887.
[27] Y. Mao, J. He, X. Sun, W. Li, X. Lu, J. Gan, Z. Liu, L. Gong, J. Chen, P. Liu, Y. Tong, Electrochim. Acta 62 (2012) 1.
[28] P.Y. Yu, Y.R. Shen, Phys. Rev. B 12 (1975) 1377.
[29] N. Tabuchi, H. Matsumura, Jpn. J. Appl. Phys. 41 (2002) 5060.
[30] H.W. Foote, E.K. Smith, J. Am. Chem. Soc. 30 (1908) 1344.
[31] M.A. Dar, S.H. Nam, Y.S. Kim, W.B. Kim, J. Solid State Electrochem. 14 (2010) 1719.